

Photochemically Patterned Poly(methyl methacrylate) Surfaces Used in the Fabrication of Microanalytical Devices

Suying Wei, Bikas Vaidya, Ami B. Patel, Steven A. Soper, and Robin L. McCarley*

Department of Chemistry and Center for Biomolecular Multi-scale Systems, Louisiana State University, 232 Choppin Hall, Baton Rouge, Louisiana 70803-1804

Received: March 25, 2005; In Final Form: May 31, 2005

We report here the photochemical surface modification of poly(methyl methacrylate), PMMA, microfluidic devices by UV light to yield pendant carboxylic acid surface moieties. Patterns of carboxylic acid sites can be formed from the micrometer to millimeter scale by exposure of PMMA through a contact mask, and the chemical patterns allow for further functionalization of PMMA microdevice surfaces to yield arrays or other structured architectures. Demonstrated here is the relationship between UV exposure time and PMMA surface wettability, topography, surface functional group density, and electroosmotic flow (EOF) of aqueous buffer solutions in microchannels made of PMMA. It is found that the water contact angle on PMMA surfaces decreases from 70° to 24° after exposure to UV light as the result of the formation of carboxylic acid sites. However, upon rinsing with 2-propanol, the water contact angle increases to approximately 80°, and this increase is attributed to changes in surface roughness resulting from removal of low molecular weight PMMA formed from scission events. In addition, the surface roughness and surface coverage of carboxylic acid groups exhibit a characteristic trend with UV exposure time. Electroosmotic flow (EOF) in PMMA microchannels increases upon UV modification and is pH dependent. The possible photolysis mechanism for formation of carboxylic acid groups on PMMA surfaces under the conditions outlined in this work is discussed.

Introduction

Biological microelectromechanical systems (BioMEMS) have attracted significant interest in recent years due to their potential impact on biological analysis, drug development, and medical diagnostics.^{1–5} The promise of BioMEMS in instrument development and assay methodologies is associated with the intrinsic advantages of BioMEMS, such as small footprint and easy multiplexing, and the potential for integration of various components into the system, as well as mass production of the devices at an attractive cost. Since the first fabrication of micro-electrophoresis devices in glass substrates using photolithography and wet chemical etching,^{5,6} various microdevices have been constructed and used for bioanalytical applications, such as PCR amplification of oligonucleotides,^{7,8} separation of single-stranded^{9–11} and double-stranded DNA,^{12–14} and protein analysis.^{15,16}

Most of the early BioMEMS devices were made of glass, quartz, or silicon because of the well-established micromanufacturing techniques and surface chemistry of silicon and silicon oxides, their rigidity, and optical properties.^{17,18} The use of polymer substrates in the construction of BioMEMS devices has become increasingly important because microstructures, including those with high aspect ratios, can be readily produced in polymers using rather straightforward processing methods.^{19,20} In addition, massive fabrication of most parts of polymer-based BioMEMS devices can be achieved using various techniques such as laser ablation,²¹ injection molding,²² hot embossing,²³ imprinting,²⁴ and soft lithography.^{25,26} Moreover, the relatively low glass transition temperature (T_g) of most polymers should make it possible to attach biomolecules before devices are assembled (thermal annealing), which cannot be achieved in SiO₂-based devices because of the high glass transition tem-

perature ($T_g > 600$ °C) of this material. Poly(methyl methacrylate), PMMA, a thermoplastic polymer, is one of the primary polymeric materials that has been used for fabrication of microanalytical devices.^{19,27,28}

Surface characteristics, such as wettability, surface topography, and interfacial charge density and distribution, are crucial factors that govern the functional capabilities of BioMEMS devices, due in part to the high surface-to-volume ratio.^{29–32} Chemical modification techniques for SiO₂-based devices are well established using silane-based chemistry,¹⁷ but a wide variety of routine, simple, and well-defined surface modification protocols for polymers used in BioMEMS applications is needed.^{28,29,33} Preformed PMMA microchannels have been modified using a pulsed UV excimer laser to reduce band broadening effects in electrophoretic separations,³⁴ and poly(carbonate) microchannels have been made “more hydrophilic” by UV irradiation.³⁵ PMMA surfaces have also been made more water wettable by direct amination,²⁹ vapor-phase deposition of organic films,³⁶ copolymer grafting,³⁷ or formation of molded devices via photo- or thermopolymerization of comonomers.^{38,39} In addition, it has been shown that PMMA surfaces can be readily patterned through techniques such as photodirected electroless deposition,⁴⁰ photoinitiated grafting,⁴¹ and exposure to deep UV sources.^{42,43} Electroosmotic flow was also controlled by either UV laser ablation in preformed PMMA microchannels or PEG grafting after PMMA surfaces were activated by oxygen plasma treatment.⁴⁵ Continued expansion of surface modification routes is essential to the development of BioMEMS technologies based on polymer substrates.

Reported here is a photochemical surface modification protocol for PMMA, a well-known substrate material for the fabrication of BioMEMS devices. It has been found that surface carboxylic acid groups are formed upon UV exposure of PMMA

* Address correspondence to this author. E-mail: tunnel@LSU.edu. Phone: +1-225-578-3239. Fax: +1-225-578-3458.

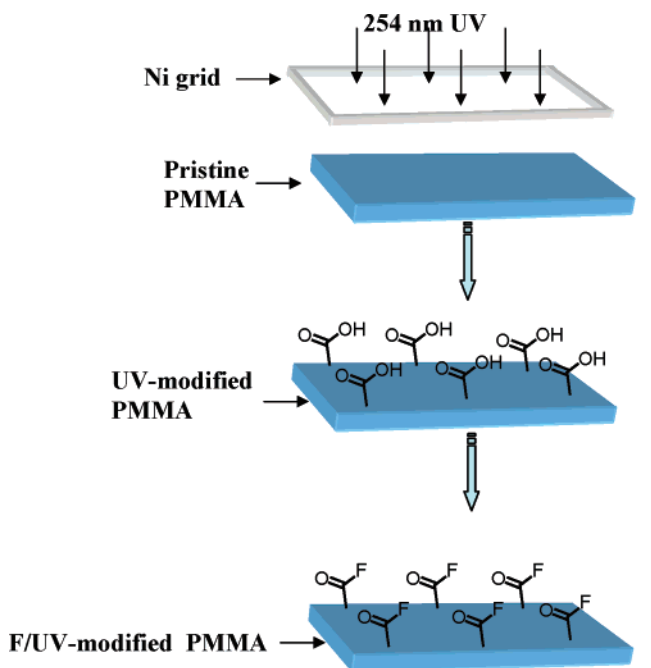
surfaces in the atmosphere (surface photochemical modification), and the resulting surface carboxylic acids allow for further functionalization of PMMA-based BioMEMS devices.⁴⁶ Surface properties of the PMMA for each step of the treatment process are systematically investigated—qualitatively and quantitatively—by water contact angle measurements, scanning force microscopy, X-ray photoelectron spectroscopy, fluorescence microscopy, and specific functional group labeling. In addition, the effect of UV modification on electroosmotic flow in hot-embossed PMMA microchannels is demonstrated. Finally, a possible mechanism for the photochemical carboxylic acid formation is discussed, based on the outcomes from deconvolution of X-ray photoelectron spectra of pristine and UV-exposed PMMA surfaces.

Experimental Section

General. Poly(methyl methacrylate) sheets, Plexiglass or Lucite, were purchased from Goodfellow and AIN and were machined to various-sized pieces. Before any type of experimental analysis was carried out, PMMA pieces were sonicated in 2-propanol (IPA) for 15 min, then rinsed with IPA and subsequently dried with a flow of house nitrogen; scanning force microscopy did not indicate any increases in surface roughness as a result of this cleaning protocol. HPLC-grade 2-propanol (IPA) and all other chemicals were obtained from Aldrich and used without any further purification unless noted otherwise. The UV light source used here is a low-pressure mercury lamp possessing an emission spectrum spanning the 240 to 425 nm range; the 254 nm band is the strongest with an intensity of 15 mW cm^{-2} , while that of all others is less than 1.5 mW cm^{-2} at a 1-cm distance. The microfluidic electrophoresis devices were fabricated using a method developed before.⁴⁷ In brief, a metal molding die, which consists of raised microstructures electroplated from Ni on a stainless steel base plate, was made using the X-ray LIGA technique.^{19,47} PMMA microstructures were embossed in a system that consisted of a PHI Precision Press (model number TS-21-H-C (4A)-5; City of Industry, CA), in which a vacuum chamber was installed to produce low pressure (<0.1 bar) for complete filing of the Ni molding die. During embossing, the molding die was heated to 150°C and pressed into the sheet PMMA at 1000 lb for 4 min. The PMMA part was then cooled to 85°C for demolding. The embossed PMMA substrate (0.5 cm thick) was annealed to a piece of PMMA cover plate (0.05 cm thick) to enclose the microfluidic channel, which was achieved by clamping both parts with glass plates and heating in a convection oven at 105°C for 15 min. To make UV-modified (carboxylic acid-modified) PMMA microchannels, the embossed PMMA substrate was first exposed to UV light for 30 min, and then rinsed with IPA. The cover plate was also processed in a similar fashion, and both PMMA pieces were then annealed at 98°C for 15 min in the oven described above. The microfluidic electrophoresis device consists of cross-flow channels with a separation channel length of 4 cm, a channel depth of $100 \mu\text{m}$, and channel width of $50 \mu\text{m}$.

Contact Angle Measurements. Sessile water contact angle measurements were used to probe the effect of UV exposure on the surface hydrophilicity of PMMA. Contact angle values on PMMA surfaces were obtained with a VCA 2000 contact angle system equipped with a CCD camera (VCA, Billerica, MA). Approximately $2 \mu\text{L}$ of deionized water ($18 \text{ M}\Omega \text{ cm}$) was placed on the PMMA surface using a syringe, and the contact angle of the water droplet was measured immediately using the software provided by the manufacturer. The measurements were repeated at least five times at separate positions on a given substrate, and the values here are reported as the mean \pm one standard deviation.

SCHEME 1: Chemical Mapping of Carboxylic Acid Functionalities with Fluoresceinyl Glycine Amide^a



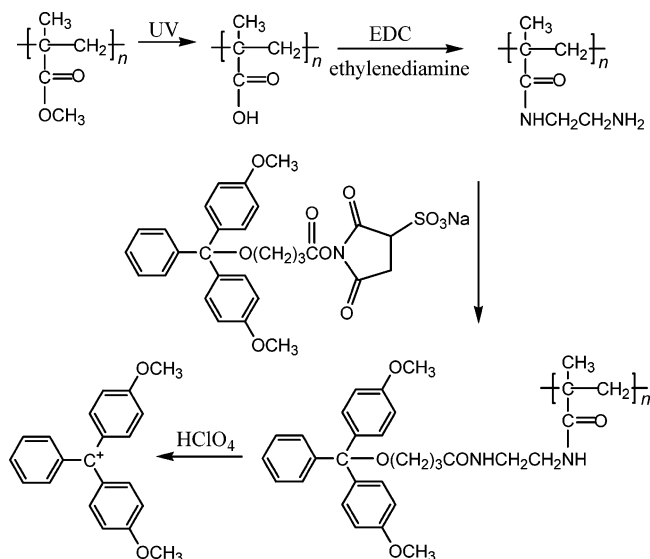
F: Fluoresceinyl glycine amide

^a PMMA was first exposed to UV light through a Photomask (2000 mesh Ni grid, with square holes of $7.6 \mu\text{m} \times 7.6 \mu\text{m}$). The groups formed as a result of exposure were derivatized with fluoresceinyl glycine amide in the presence of EDC to produce fluorescence.

Scanning Force Microscopy (SFM). The surface topographies of the pristine/unmodified and UV-modified PMMA surfaces were assessed using a Digital Instruments Nanoscope III multimode scanning force microscope in noncontact (Tapping) force mode. The images presented were treated by use of the flatten algorithm using the Nanoscope software. Root-mean-square (rms) roughness was calculated using the software provided by the instrument vendor.

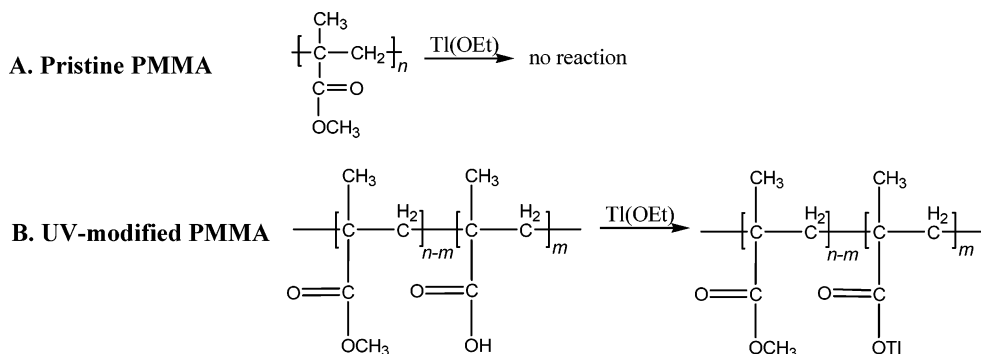
Chemical Mapping of the Functionalities Induced by Photolysis on the PMMA Surfaces. The protocol is outlined in Scheme 1 and is as follows. A piece of PMMA sheet ($2.54 \text{ cm} \times 7.62 \text{ cm} \times 0.05 \text{ cm}$ from AIN Plastics) was ultrasonicated in 2-propanol for 15 min, rinsed with 2-propanol (IPA), and dried with house N_2 . The sample was placed on a microscope slide and a 2000 mesh Ni grid (SPI; hole size of $7.6 \mu\text{m}$ and wire size of $5 \mu\text{m}$) held on the sample with an Al dumbbell-shaped mask.⁴⁸ The piece of PMMA was placed under the UV lamp for 30 min. Next, the PMMA was rinsed with 2-propanol (IPA) and dried with house nitrogen. The UV-modified PMMA sheet was immersed in 0.5 mM *N*-ethyl-*N'*-(3-dimethylamino-propyl)carbodiimide (EDC) + 0.5 mM fluoresceinyl glycine amide (Molecular Probes) in pH 7.0, 100 mM phosphate buffer. Then, the immersed PMMA was placed on a slow shaker to react overnight. The PMMA sheet was rinsed with pH 7.0 phosphate buffer and dried by tilting onto a Kim Wipe. Fluorescence images were then immediately taken with a Nikon Photoshot Fx fluorescence microscope. The excitation and the emission filters used were 488 and 520 nm, respectively.

Determination of Surface Carboxylate Concentration. As is illustrated in Scheme 2, a protocol taken from Pierce Biotechnology, Inc. was used to measure the surface coverage of carboxylic acid groups. This protocol of course assumes

SCHEME 2: Quantification of Carboxylic Acid Groups on UV-Modified PMMA Surfaces Using the Trityl Cation Method^a


^a PMMA sheets were first exposed to UV radiation and then the induced functional groups were derivatized with ethylenediamine in the presence of EDC to yield an amine-terminated surface. The amine-terminated surfaces were then reacted with s-SDTB (sulfo-succinimidy-4-O-(4,4'-dimethoxytrityl)butyrate), and then subsequently exposed to perchloric acid to release into solution the trityl cation from the PMMA surface, which absorbs strongly at 498 nm.

100% efficiency for each step (amine coupling and tritylcarboxylic acid coupling). The procedure can be described as follows. Samples were prepared by ultrasonication of the PMMA sheets in IPA for 15 min, rinsing with IPA, and then drying under house N₂ flow. The cleaned PMMA samples were then exposed to UV light in the atmosphere for different periods of time, rinsed with IPA, and dried under house N₂ flow. Each UV-modified PMMA sheet was placed in a capped vial, and 2 mL of EDC solution (5 mM in pH 7.0, 0.1 M phosphate buffer) and 30 μ L of ethylenediamine were added to each vial. All vials were placed on a shaker table to react for 3 h, after which each sample was rinsed thoroughly with 18 M Ω cm water, then placed in a precleaned glass vial containing 2 mL of freshly prepared sulfo-succinimidy-4-O-(4,4'-dimethoxytrityl)butyrate (s-SDTB) solution (0.1 mM), and reacted on a shaker for 30 min. At this point, each sample sheet was rinsed thoroughly with 18 M Ω cm water, placed in a precleaned vial containing 2 mL of perchloric acid solution (51.4 mL of 70% perchloric acid + 46.0 mL of 18 M Ω cm), and ultrasonicated for 15 min. The absorbance of the solution in each vial was then measured at 498 nm with a Cary 50 UV-vis spectrometer.

SCHEME 3: Ti⁺ Labeling of COOH Functionalities on Pristine and UV-Modified PMMA Surfaces As Reported by Batich et al.⁵¹


Electroosmotic Flow Measurement. PMMA microchannels (4 cm long, 100 μ m tall, and 50 μ m wide) were formed by hot-embossing with the embossing system (vide infra) and the microchannel was enclosed by thermal annealing as described above.⁴⁹ The electroosmotic flow (EOF) was measured by the well-established current monitoring method,⁵⁰ described as follows. The microchannel and both reservoirs were first filled with a low concentration buffer, one reservoir was subsequently emptied and filled with a higher concentration buffer, or vice versa. The ionic strengths of the buffers were kept to within 10% of each other (18–20 mM) so as to minimize double layer compression effects.⁵⁰ Electrodes were placed in the reservoirs, then a high voltage (600 V) was applied across the 4-cm channel, and the current was monitored by following, with a multimeter (Fluke 189), the voltage drop across a 10 K Ω resistor connected into the circuit. EOF values were measured using 10.0 and 20.0 mM acetate buffer in the pH range of 4–6, 10.0 and 20.0 mM phosphate buffer in the pH range of 7–8, and 10.0 and 20.0 mM borate buffer in the pH range of 9–10. In these measurements, the voltages from the multimeter were uploaded in real time to a computer in which the Flukeview 2.0 program (Fluke) was installed.

Element-Specific Labeling of PMMA Surfaces and Analysis with X-ray Photoelectron Spectroscopy. As previously shown⁵¹ and is outlined in Scheme 3, Ti(OEt)₄ will specifically react with carboxylic acid groups while not ester groups, so the amount of Ti coupled to the polymer surfaces will indicate the number of accessible carboxylic acid groups on the polymer surfaces. Ti(OEt)₄ exposure of pristine PMMA, UV-modified PMMA, and poly(methacrylic acid), PMAA (Scientific Polymer Products, Inc., M_w = 87 100 and PDI = 1.02), was accomplished by placing the polymer spin-coated glass microscope slides in an Ar-filled glovebox (Vacuum Atmospheres) and covering them with neat Ti(OEt)₄ liquid (Strem Chemical, Inc.) for 30 s, rinsing with absolute ethanol, and drying completely. The Ti-exposed slides were then analyzed with an Axis 165 X-ray photoelectron spectrometer (Kratos Analytical) using a monochromatized Al K α (1486.6 eV) X-ray source with a power of 150 W. Survey and high-resolution spectra were obtained using pass energies of 160 and 20 eV, respectively. The neutralizer was turned on during the analysis to compensate for any possible charge effects on the insulating polymer surfaces. Core level binding energies for C1s and O1s were corrected according to Beamson et al. referencing the methyl carbons to 285.0 eV and carbonyl oxygens to 532.2 eV, respectively.⁵²

Curve-fitting of the high-resolution spectra of the Ti-labeled pristine and UV-modified PMMA was used for mechanistic analysis of the possible photochemical reactions described herein. The curve fitting was performed using a sum of

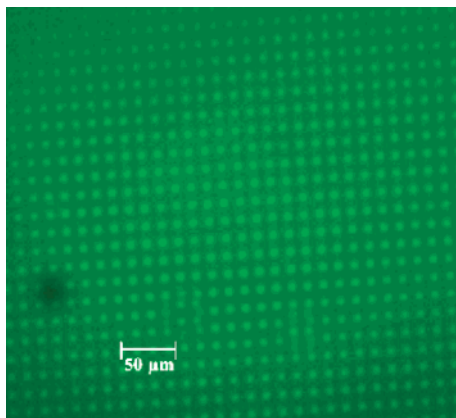


Figure 1. Image of photopatterned PMMA surface; here a 2000 mesh Ni grid was used as a mask (7.6 micron squares), exposure time is 30 min. Fluorescence image ($\lambda_{\text{ex}} = 488 \text{ nm}$, $\lambda_{\text{em}} = 520 \text{ nm}$) of specific chemical labeling with fluoresceinyl glycine amide.

Gaussian–Lorentzian profile peak shapes after subtraction of a linear background.⁵²

Results and Discussion

Fluorescence Microscopic Mapping of Carboxylic Acid Functionalities on UV-Exposed PMMA Surfaces. Chemical labeling of carboxylic acid groups on PMMA surfaces followed by their examination with fluorescence microscopy was used to identify the presence of carboxylic acid groups formed during the photolysis process on the PMMA surfaces. As can be seen from Scheme 1, fluoresceinyl glycine amide, in the presence of carbodiimide coupling agent, specifically reacts with carboxylic acids on the PMMA surfaces to form amide bonds. This dye has been used previously in mapping carboxylic acid sites in acrylate-based polymer microfluidic devices.⁵³ Shown in Figure 1 is a fluorescence image ($\lambda_{\text{excit}} = 488 \text{ nm}$, $\lambda_{\text{emis}} = 520 \text{ nm}$) of fluoresceinyl glycine amide dye-conjugated PMMA surfaces after being patterned by UV modification using a 2000 mesh Ni grid (hole size of $7.6 \mu\text{m}$) as a mask for 30 min. As

outlined in the Experimental Section, the green squares in Figure 1 are where the UV modification was performed and therefore the green dye should be present. Control experiments on UV-exposed PMMA without EDC did not lead to observation of fluorescence signal. The images obtained from these experiments indicate that carboxylic acid groups are formed on UV-modified PMMA surfaces using the protocol described here.

Surface Topographic Analysis of Pristine and UV-Modified PMMA Using SFM. Surface topography is an important issue for substrate support materials used in applications such as biosensors and microanalytical devices, to name a few.^{32,54} In particular with microfluidic devices, small changes in substrate surface roughness upon chemical treatment are desired due to the size of the device features (μm). In this study, SFM was used to analyze both pristine and UV-modified PMMA surfaces. In general, UV-modified PMMA surfaces are slightly rougher than the pristine PMMA surfaces, as can be noted from inspection of Figure 2 and Table 1. Figure 2A represents a typical $20 \mu\text{m} \times 20 \mu\text{m}$ SFM image of the surface of pristine 0.5-mm-thick PMMA sheets (Goodfellow), with the surface being relatively uniform and smooth; the rms surface roughness is 18.0 nm, and the roughness factor, R , is 1.014 (R refers to the ratio of the surface cross-sectional distance to the horizontal distance²⁹). Shown in Figure 2B is a typical $20 \mu\text{m} \times 20 \mu\text{m}$ SFM image of a 0.5-mm-thick Goodfellow PMMA sheet that was UV modified for 30 min under ambient laboratory atmosphere, subsequently rinsed with IPA, and then dried with house N_2 . The rms surface roughness for the 30-min, UV-modified PMMA surface is 27.5 nm, which is about 50% higher than that of the pristine PMMA, and the roughness factor R is 1.067. This increased surface roughness is attributed to photo-induced scission reactions of the polymer chains on the PMMA surfaces.⁵⁵ Preliminary mass spectrometry studies of 1° standard PMMA photochemically modified under the conditions described here confirm this scission pathway is operative. However, under the conditions used here (15 mW cm^{-2} , $t < 2 \text{ h}$), the photochemical surface modification route (carboxylic acid

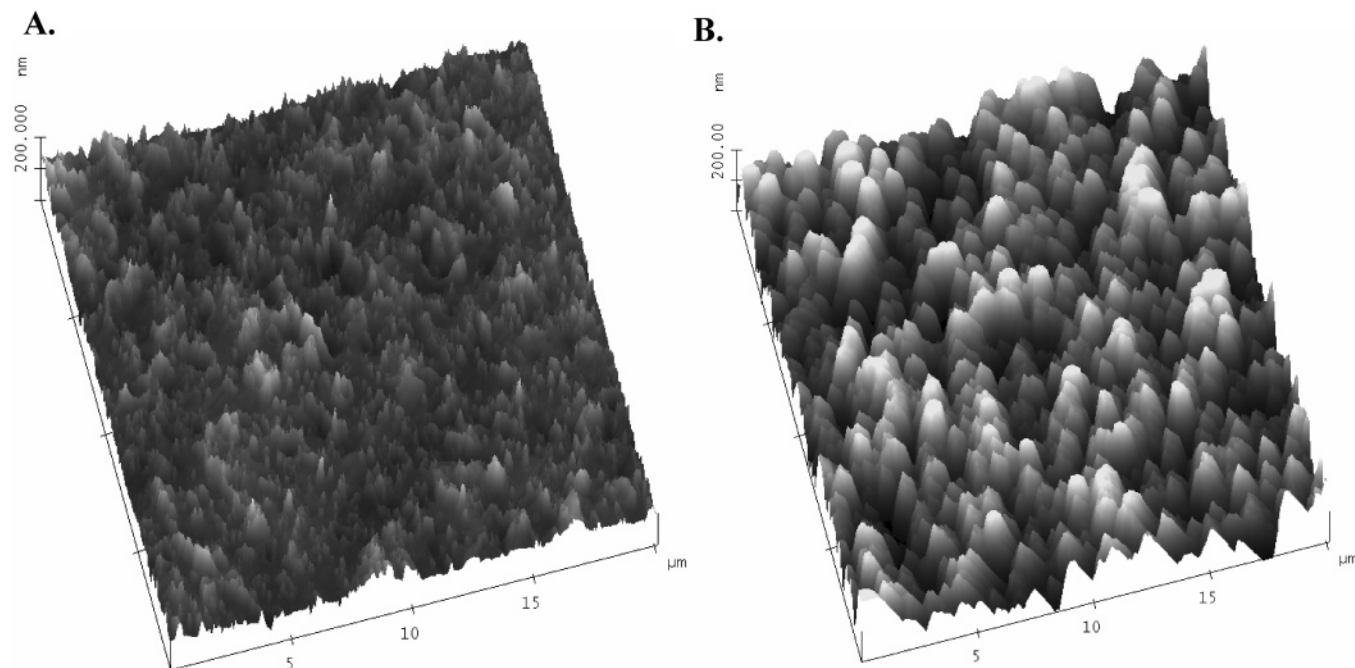


Figure 2. Tapping mode SFM images of (A) pristine PMMA and (B) UV-modified PMMA (30 min). The scan range for both images is $20 \mu\text{m} \times 20 \mu\text{m}$, and the Z-range is 200 nm. Root-mean-square (rms) surface roughness is 18 nm for pristine PMMA while it is 27.5 nm for the UV-modified PMMA. The surface area correcting factor R value for the pristine PMMA is 1.014, while it is 1.067 for the 30-min, UV-exposed PMMA.

TABLE 1: Values of Carboxylic Acid Surface Coverage Resulting from Photochemical Surface Modification of PMMA as a Function of Modification Time (three replicates, confidence interval = 90%)^a

	UV modification time (min)					
	0	5	10	30	60	121
rms surface roughness (nm)	18.0 ± 0.9	14.8 ± 0.4	41.1 ± 0.8	27.5 ± 0.5	33.0 ± 0.2	32.3 ± 0.7
correction factor (<i>R</i>) for surface area	1.014 ± 0.008	1.008 ± 0.003	1.317 ± 0.007	1.067 ± 0.005	1.042 ± 0.001	1.094 ± 0.006
surface coverage of COOH (10 ⁻¹⁰ mol·cm ⁻²) before correction for surface roughness	0.47 ± 0.01	3.02 ± 2.80	8.57 ± 0.48	13.97 ± 0.55	14.13 ± 0.99	16.83 ± 0.28
surface coverage of COOH (10 ⁻¹⁰ mol·cm ⁻²) after correction for surface roughness	0.46 ± 0.02	3.00 ± 1.32 (50%) or 3.00 ± 4.72	6.61 ± 0.81	13.12 ± 0.93	13.44 ± 1.67	15.53 ± 0.47

^a Note: for the 5-min exposure, we obtained 3.00 ± 1.32 at a confidence interval of 50% and 3.00 ± 4.72 at a confidence interval of 90%. The plot in Figure 4 used the former data (3.00 ± 1.32).

formation) is dominant, as noted by the relatively small change in roughness values. For the longest exposure time, we find an rms roughness of 32.3 nm and $R = 1.094$. We currently do not understand the origin of the high roughness values for the 10-min exposure. All in all, the observed roughness increase upon photochemical surface modification is quite small, particularly in light of the dimensions of the microchannels.

Sessile-Drop Water Contact Angle Measurements of Pristine and UV-Modified Poly(methyl methacrylate) Surfaces. The average contact angle for pristine PMMA surfaces using water as the probe was found to be $70^\circ \pm 2^\circ$ (5 replicates), in good agreement with the literature value of 67° .^{29,56} After photochemical surface modification in air, but before IPA rinsing, the water contact angle is decreased to about 24° at 30 min exposure time, see Figure 3. When the photochemically modified surfaces were rinsed with IPA, the water contact angle values increased, possibly as a result of increased surface roughness caused by IPA removal⁵⁷ of low molecular weight polymers⁵⁵ on the PMMA surfaces formed during the photochemical modification process. When PMMA surfaces are exposed to UV light, the radical ends resulting from bond breaking events in the irradiated volume can be trapped by oxygen in the atmosphere to form initial oxidation products which can undergo further photolysis to give smaller fragments.⁵⁵ We hypothesize that the nanoscale roughness causes the increase in contact angle in a fashion similar to that recently observed for nanostructured polymer surfaces that mimic biological surfaces.⁵⁸

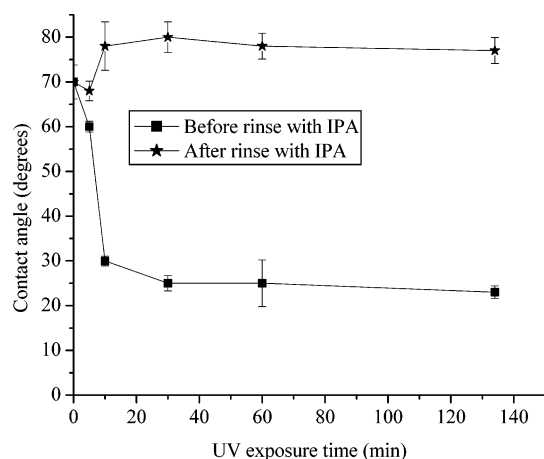


Figure 3. Effects of UV modification on the water contact angle on PMMA surfaces. Water contact angle was measured on PMMA surfaces that were UV modified in air for different UV exposure times both before rinsing with IPA (solid squares) and after rinsing with IPA (solid stars). The water contact angle was measured immediately after each treatment to avoid any possible contamination from the atmosphere.

Determination of Surface Coverage of Carboxylic Acid Groups on PMMA by Visible Dye Labeling. UV-vis spectrometry coupled to carboxylic acid group-specific labeling was used to quantify the surface coverage of carboxylic acid functionalities on UV-modified PMMA surfaces, Scheme 2. Before photochemical surface modification, there exists a small number of carboxylic acid sites on the pristine PMMA, see Table 1 and Figure 4. This is attributed to hydrolysis of the surface PMMA ester groups by either the manufacturer production or post-manufacturer production conditions of the polymer before its purposeful photochemical modification. The surface concentration of carboxylate groups on PMMA surfaces was found to increase consistently with increases in the photochemical modification time up to 30 min, and then it tended toward a limiting value, as seen in Figure 4. The surface coverage of carboxylic acid sites on PMMA surfaces reaches 1.68 nmol cm⁻² at a modification time of 2 h, which upon correction for surface roughness (Table 1, R value) is 1.55 nmol cm⁻², a value that is ~ 1.5 – 2 times that of a close-packed alkane monolayer.⁵⁹ This higher-than-monolayer coverage is most likely due to the formation of carboxylic acid groups below the PMMA surface, an expected outcome based on the photochemical modification protocol (vide supra).

Effect of Photoinduced Carboxylic Acid Presence on Electroosmotic Flow in PMMA Microchannels. Electroosmotic flow has been discussed recently in regards to its magnitude and direction for chemically modified PMMA microchannels made through machining²⁹ and by laser-ablation.²⁴ To investigate the effect on EOF of carboxylic acid

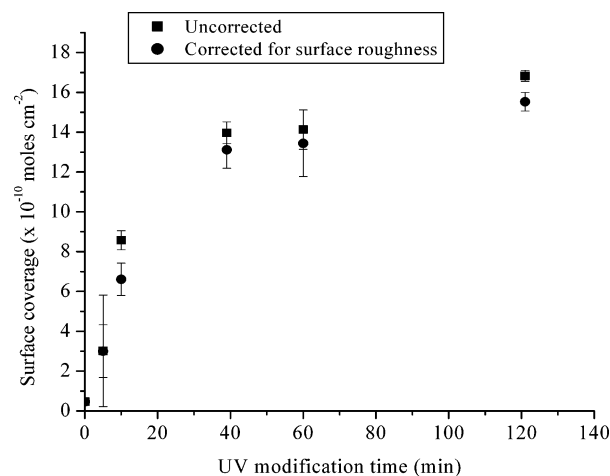


Figure 4. Surface coverage of carboxylic acids as a function of UV exposure time for PMMA surfaces in ambient air. Values uncorrected (solid squares) and corrected (solid circles) for SFM-determined roughness are reported.

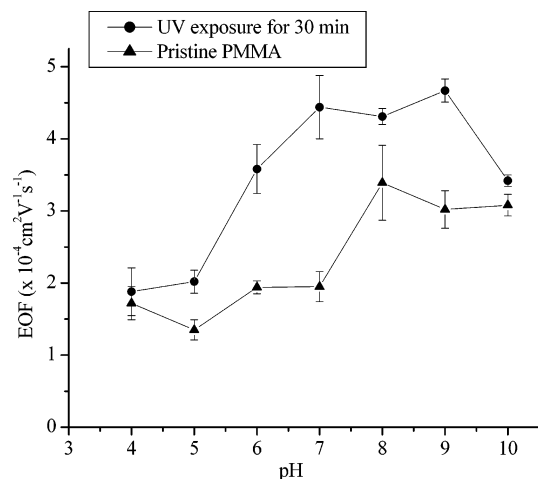


Figure 5. Electroosmotic flow measurements in a hot-embossed PMMA microchannel ($4 \text{ cm} \times 100 \mu\text{m} \times 50 \mu\text{m}$). Plot of EOF vs pH for pristine (solid triangles) and 30-min UV-modified PMMA (solid circles). The electroosmotic flow measurements were carried out using pH values of 4–10. Three different buffers were used: acetate buffer (pH 4.0, 5.0, and 6.0); phosphate buffer (pH 7.0 and 8.0); and borate buffer (pH 9.0 and 10.0). The concentration of buffer was held between 18 and 20 mM, while the field strength used was 150 V cm^{-1} . For the modified materials, the microchannels of the embossed PMMA were exposed prior to chip assembly through use of a mask.

groups resulting from photochemical surface modification, a microchannel ($100 \mu\text{m}$ deep, $50 \mu\text{m}$ wide, 4 cm long) was hot embossed in PMMA and subsequently irradiated as described here for 30 min, rinsed with IPA, and dried with house N_2 , and then the microchannel was enclosed by thermal bonding with a piece of pristine PMMA cover plate to form a fluidic conduit.^{18,47,60} As is seen in Figure 5, the EOF in both pristine and UV-modified PMMA microchannels is positive (from anode to cathode) and changes with the pH value of the buffer used. For example, the EOF values increased at higher pH for both photochemically modified ($4.67 \times 10^{-4} \text{ cm}^2 \text{ V}^{-1} \text{ s}^{-1}$ at pH 9.0 and $1.88 \times 10^{-4} \text{ cm}^2 \text{ V}^{-1} \text{ s}^{-1}$ at pH 4.0) and pristine PMMA microchannels ($3.02 \times 10^{-4} \text{ cm}^2 \text{ V}^{-1} \text{ s}^{-1}$ at pH 9.0 and $1.72 \times 10^{-4} \text{ cm}^2 \text{ V}^{-1} \text{ s}^{-1}$ at pH 4.0), and this is attributed to the fact that the accessible surface carboxylic acids are deprotonated at high pH and protonated at low pH values. In general, the EOF values in photochemically modified PMMA microchannels are higher than those in pristine PMMA microchannels, an observation that is consistent with the presence of a higher surface density of solution-accessible carboxylic acid moieties. This increased amount of carboxylic acid sites results from the photochemical modification process. Thus, the photochemically modified PMMA surfaces possess more ionizable functional groups than their pristine counterparts. In addition, the significant change in EOF with pH change occurs at a lower pH value for UV-modified PMMA microchannels (pH ~ 6.0), while this is observed at a higher pH value for pristine PMMA microchannels (pH ~ 7.0). This observation is most likely related to the issue of surface pK_a and its dependence on ionizable group surface density, although further work is needed to gain a better understanding of this phenomenon.

Mechanism for the Photochemical Surface Modification of PMMA-XPS Studies. As a powerful surface analysis technique, XPS is able to provide information on the chemical changes in the very top layer of the PMMA sample where photochemical reactions occur.⁴² The XPS data in Table 2 demonstrate that the ratio of O/C on PMMA surfaces increases when the UV modification time of PMMA surfaces in air is increased, which indicates that introduction of oxygen into the

TABLE 2: XPS Quantification Data of Elemental Composition of Carbon, Oxygen, and the Ratio of These Two Elements in Accordance to UV Modification Time on PMMA Surfaces (three replicates, confidence interval = 90%)

exposure time (min)	atomic conc (%)			
	C1s	O1s	O1s/C1s	av of O1s/C1s
0	77.17	22.83	0.296	0.292 ± 0.009
	77.77	22.23	0.286	
	77.31	22.69	0.293	
10	75.12	24.88	0.331	0.335 ± 0.007
	74.81	25.19	0.337	
	74.74	25.26	0.338	
30	74.71	25.29	0.339	0.340 ± 0.003
	74.47	25.53	0.343	
	74.69	25.31	0.339	
60	73.75	26.25	0.356	0.356 ± 0.002
	73.82	26.18	0.355	
	73.72	26.28	0.356	
120	74.17	25.83	0.348	0.349 ± 0.007
	74.34	25.66	0.345	
	73.93	26.07	0.353	

TABLE 3: Comparison of XPS Data on Different Polymer Films Treated with Tl(OEt)

atomic ratio	C1s/O1s	Tl4f/O1s	coverage of COOH (%)
Tl/pristine PMMA	2.79 ± 0.20	0.040 ± 0.002	11 ± 2
Tl/UV-modified (30 min) PMMA	2.60 ± 0.07	0.14 ± 0.01	39 ± 2
Tl/standard PMAA	1.98 ± 0.11	0.36 ± 0.02	100 ± 2

polymer occurs during UV modification of PMMA surfaces as described here. This observation is also consistent with the results from the chemical labeling (trityl cation, Scheme 2) of the carboxylic acid functionalities of photochemically modified PMMA surfaces, as it was observed that more carboxylic acid sites were formed with increased modification time, Figure 4.

To identify the presence of and provide a semiquantitative evaluation of the amount of carboxylic acid sites on the UV-exposed PMMA, we employed a carboxylic acid-selective labeling method, Scheme 3.⁵¹ Thallium ethoxide has been shown to be effective for semiquantitatively labeling carboxylic acids on polymeric surfaces.⁵¹ Here, neat thallium ethoxide was used to probe the presence of surface carboxylic acid groups on pristine PMMA, UV-modified PMMA, and poly(methacrylic acid), PMAA (as a reference) surfaces, and the atomic ratio of Tl/O was obtained for each surface. The Tl/O values were used to obtain approximate carboxylic acid surface coverage values upon comparison to a surface that should possess the maximum number of carboxylic acid sites, namely, poly(methacrylic acid), PMAA, which we arbitrarily assign as a 100% carboxylic acid layer. These surface coverage values are only a rough estimate and should not be compared to those from the trityl-labeling route above, for they do not reflect the labeling efficiency and the tacticity of the polymeric material used (the PMMA is mainly a syndiotactic isomer based on our preliminary NMR results, whereas the PMAA possesses a tacticity that is somewhere between isotactic and syndiotactic), and the depth to which the Tl(EtO) penetrates is possibly different for PMAA and PMMA. Furthermore, as pointed out by Batich et al., the method works best for surface coverages of carboxylic sites that are less than $\sim 30\%$ of a monolayer.⁵¹ As noted in Table 3, the photochemically modified PMMA surface possesses a much higher carboxylic acid surface coverage compared to its pristine counterpart (about 3.5 times), in general agreement with the trend observed with the trityl-labeling route (Scheme 2, Table 1).

TABLE 4: Comparison of the Deconvoluted XPS Spectra of Pristine and Photochemically Modified (30 min) PMMA^a

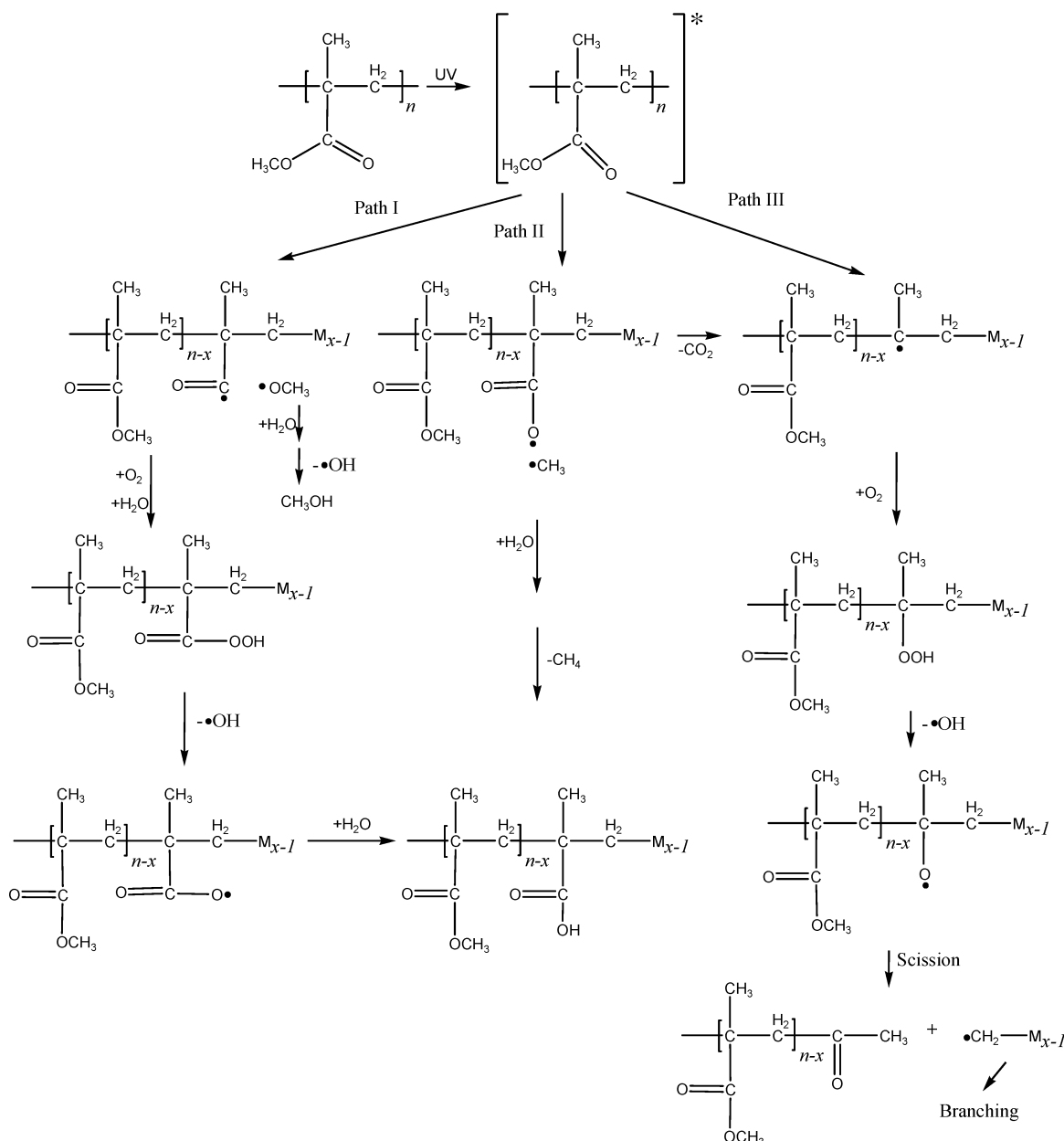
O1s peak label in Figure 6	position BE (eV)	atomic conc %	
		pristine PMMA	UV-modified PMMA
<i>b</i>	530.50	3.4	19.4
<i>c</i>	532.20	46.4	44.5
<i>a</i>	533.70	50.2	36.1

^a Curve fitting was achieved by application of a Gaussian–Lorentzian peak shape algorithm (70% Gaussian and 30% Lorentzian) after subtraction of a linear background. A relative sensitivity factor of 0.780 for oxygen was used in all cases.

To provide insight to the photochemical surface modification mechanism—that is identification and quantification of oxygen-containing species possessing carboxylic acid functionalities—analysis of the deconvoluted O1s region of the X-ray photoelectron spectra for pristine and 30-min UV-modified PMMA

surfaces was undertaken, Table 4 and Figure 6. The O1s signal denoted by *b* in Figure 6 corresponds to the carboxylic oxygen (associated with Ti^+ from labeling), that by *c* the O1s for the carbonyl oxygen, and that by *a* the O1s of the methoxyl oxygen. It is clearly seen that the amount of methoxyl oxygen (*a*) decreased (from 50.2% to 36.1%) while the amount of carboxylic oxygen (*b*) increased (from 3.4% to 19.4%) upon photochemical modification, indicating that the methoxyl group is cleaved and the free carboxylic acid is formed during UV modification.

A proposed PMMA photolysis mechanism for the conditions described in this report is shown in Scheme 4 and is based on others proposed in the literature.^{61,62} As is illustrated in Scheme 4, PMMA is first raised to the excited state upon absorption of UV light, and then it can undergo three possible pathways to form different radical products. These three pathways may occur simultaneously. In Path I, carbonyl and methoxyl radicals are formed, the latter which will extract hydrogen (from water or

SCHEME 4: Proposed Mechanism for the Photochemical Surface Modification Reaction under the Conditions Described Here^a

^a Adapted from previous work.^{61,62}

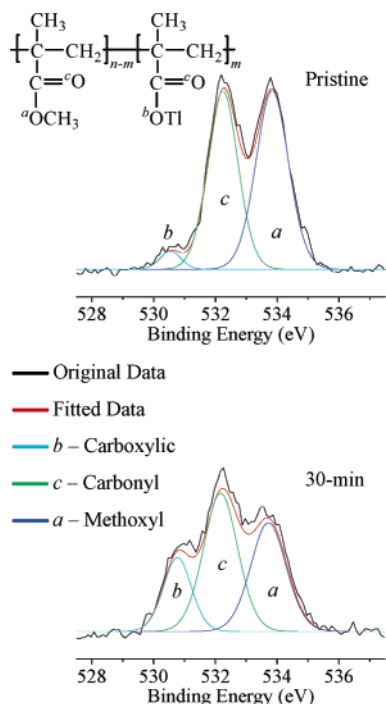


Figure 6. Deconvoluted X-ray photoelectron spectra in the O1s region for pristine and 30-min, UV-modified PMMA: (Top) pristine PMMA after exposure to Ti(OEt) and (Bottom) 30-min UV-modified PMMA after exposure to Ti(OEt). There are three components for both spectra, designated as (c) carbonyl oxygen, (a) methoxyl oxygen, and (b) carboxylic oxygen (bound to Ti⁺).

the polymer itself) to yield methanol, while the carbonyl radical will form a peracid in the presence of oxygen and UV light, which in turn will lead to carboxyl radicals that react with water to yield a polymer-bound carboxylic acid. In Path II, methyl and carboxyl radicals are formed, which react with water to yield methane and a polymer-bound carboxylic acid. In Path III, tertiary carbon radicals are produced directly from the excited state or when the carboxyl radicals in Path II release carbon dioxide. Then, in the presence of oxygen, the tertiary carbon radicals may further form alkoxy radicals (through a peroxide intermediate), which in turn lead to polymer chain scission with the formation of acetone and alkyl radical on the scissed polymer chain; the latter may possibly undergo polymer chain branching reactions.^{61,62} It is clear that Path III is operative to some degree in the work at hand, as noted by the small increase in PMMA surface roughness with exposure time (removal of scission polymer product with IPA rinsing) and preliminary mass spectrometry data (vide supra); however, it is not the major path. Both Paths I and II lead to the formation of carboxylic acid sites, but it is currently unclear if a given path is dominant. The surface labeling and XPS data support the carboxylic acid formation Paths I and II, but not the specific intermediates. Previous work supports the latter.^{61,62}

Conclusions

This report focuses on the surface modification of PMMA with simple UV photochemical methods, during which roughly a monolayer of carboxylic functional groups is formed. Formation of the carboxylic acids is a relatively nondestructive surface process from a physical point of view, as judged from scanning force microscopy studies, and is a very important characteristic for applications requiring minimal surface damage. The carboxylic acid groups on the PMMA surfaces lead to increases in its water wettability and the pH-dependent electroosmotic

flow in hot-embossed microchannels. In addition, the pendant carboxylic groups on PMMA surfaces make it possible to further functionalize PMMA-based BioMEMS devices. A possible photolysis process mechanism was proposed based on literature reports and outcomes from the studies presented here. Polymer-based BioMEMS devices have attracted increased interest because of their intrinsic advantages, such as ease of fabricating high aspect ratio features and their low cost, biocompatibility, and favorable mechanical properties. However, simple and convenient surface modification techniques are needed to push these microdevices ahead into the needed applications. The work described here provides a new avenue for the “bulk” surface modification of polymer-based BioMEMS devices, and more importantly, the spatially controlled modification of polymer surfaces that are required for protein and nucleic acid arrays, electronic interconnects, and localized fluid control.

Acknowledgment. This work was supported by grants from the National Science Foundation (CHE-0108961, EPS-0346411, DBI-0138048, ENG-0139656 (REU Program), and DMR-0116757) and the National Institutes of Health (R24CA842625, R21CA099246, and R01HG001499). The authors would like to acknowledge Dr. Chris Moffitt, an applications specialist from Kratos Analytical, Inc., who helped with protocols for deconvolution of X-ray photoelectron spectra.

References and Notes

- (1) Auroux, P.-A.; Iossifidis, D.; Reyes, D. R.; Manz, A. *Anal. Chem.* **2002**, *74*, 2637–2652.
- (2) Reyes, D. R.; Iossifidis, D.; Auroux, P.-A.; Manz, A. *Anal. Chem.* **2002**, *74*, 2623–2636.
- (3) Ismagilov, R. F. *Angew. Chem.* **2003**, *42*, 4130–4132.
- (4) Landers, J. P. *Anal. Chem.* **2003**, *75*, 2919–2927.
- (5) Harrison, D. J.; Fluri, K.; Seiler, K.; Fan, Z.; Effenhauser, C. S.; Manz, A. *Science* **1993**, *261*, 895–897.
- (6) Harrison, D. J.; Manz, A.; Fan, Z.; Luedi, H.; Widmer, H. M. *Anal. Chem.* **1992**, *64*, 1926–1932.
- (7) Cheng, J.; Shoffner, M. A.; Mitchelson, K. R.; Kricka, L. J.; Wilding, P. J. *J. Chromatogr. A* **1996**, *732*, 151–158.
- (8) Belgrader, P.; Young, S.; Yuan, B.; Primeau, M.; Christel, L. A.; Pourahmadi, F.; Northrup, M. A. *Anal. Chem.* **2001**, *73*, 286–289.
- (9) Shi, Y.; Simpson, P. C.; Scherer, J. R.; Wexler, D.; Skibola, C.; Smith, M. T.; Mathies, R. A. *Anal. Chem.* **1999**, *71*, 5354–5361.
- (10) Effenhauser, C. S.; Bruin, G. J.; Paulus, A. *Electrophoresis* **1997**, *18*, 2203–2213.
- (11) Salas-Solano, O.; Schmalzing, D.; Koutny, L.; Buonocore, S.; Adourian, A.; Matsudaira, P.; Ehrlich, D. *Anal. Chem.* **2000**, *72*, 3129–3137.
- (12) Woolley, A. T.; Sensabaugh, G. F.; Mathies, R. A. *Anal. Chem.* **1997**, *69*, 2181–2186.
- (13) Jacobson, S. C.; Ramsey, J. M. *Anal. Chem.* **1996**, *68*, 720–723.
- (14) Schmalzing, D.; Koutny, L.; Adourian, A.; Belgrader, P.; Matsudaira, P.; Ehrlich, D. *Proc. Natl. Acad. Sci. U.S.A.* **1997**, *94*, 10273–10278.
- (15) Liu, Y.; Foote, R. S.; Jacobson, S. C.; Ramsey, R. S.; Ramsey, J. M. *Anal. Chem.* **2000**, *72*, 4608–4613.
- (16) Sato, K.; Tokeshi, M.; Kimura, H.; Kitamori, T. *Anal. Chem.* **2001**, *73*, 1213–1218.
- (17) Silberzan, P.; Leger, L.; Ausserre, D.; Benattar, J. J. *Langmuir* **1991**, *7*, 1647–1651.
- (18) Ford, S. M.; Kar, B.; McWhorter, S.; Davies, J.; Soper, S. A.; Klopff, M.; Calderon, G.; Saile, V. *J. Microcolumn Sep.* **1998**, *10*, 413–422.
- (19) Soper, S. A.; Ford, S. M.; Qi, S.; McCarley, R. L.; Kelly, K.; Murphy, M. C. *Anal. Chem.* **2000**, *72*, 642A–651A.
- (20) Becker, H.; Heim, U. *Sens. Actuators, A* **2000**, *83*, 130–135.
- (21) Waddell, E. A.; Locascio, L. E.; Kramer, G. W. *J. Lab. Autom.* **2002**, *7*, 78–82.
- (22) McCormick, R. M.; Nelson, R. J.; Alonso-Amigo, M. G.; Benvenegut, D. J.; Hooper, H. H. *Anal. Chem.* **1997**, *69*, 2626–2630.
- (23) Qi, S.; Liu, X.; Ford, S.; Barrows, J.; Thomas, G.; Kelly, K.; McCandless, A.; Lian, K.; Goettert, J.; Soper, S. A. *Lab. Chip* **2002**, *2*, 88–95.
- (24) Locascio, L. E.; Perso, C. E.; Lee, C. S. *J. Chromatogr. A* **1999**, *857*, 275–284.
- (25) Quake, S. R.; Scherer, A. *Science* **2000**, *290*, 1536–1540.
- (26) Ng, J. M. K.; Gitlin, I.; Stroock, A. D.; Whitesides, G. M. *Electrophoresis* **2002**, *23*, 3461–3473.

- (27) Boone, T. D.; Fan, Z. H.; Hooper, H. H.; Ricco, A. J.; Tan, H.; Williams, S. J. *Anal. Chem.* **2002**, *74*, 78A-86A.
- (28) Becker, H.; Locascio, L. E. *Talanta* **2002**, *56*, 267-287.
- (29) Henry, A. C.; Tutt, T. J.; Galloway, M.; Davidson, Y. Y.; McWhorter, C. S.; Soper, S. A.; McCarley, R. L. *Anal. Chem.* **2000**, *72*, 5331-5337.
- (30) Soper, S. A.; Henry, A. C.; Vaidya, B.; Galloway, M.; Wabuyele, M.; McCarley, R. L. *Anal. Chim. Acta* **2002**, *470*, 87-99.
- (31) Vaidya, B.; Soper, S. A.; McCarley, R. L. *Analyst* **2002**, *127*, 1289-1292.
- (32) Lahann, J.; Balcells, M.; Lu, H.; Rodon, T.; Jensen, K. F.; Langer, R. *Anal. Chem.* **2003**, *75*, 2117-2122.
- (33) Belder, D.; Ludwig, M. *Electrophoresis* **2003**, *24*, 3595-3606.
- (34) Johnson, T. J.; Ross, D.; Gaitan, M.; Locascio, L. E. *Anal. Chem.* **2001**, *73*, 3656-3661.
- (35) Liu, Y.; Ganser, D.; Schneider, A.; Liu, R.; Grodzinski, P.; Kroutchinina, N. *Anal. Chem.* **2001**, *73*, 4196-4201.
- (36) Hiratsuka, A.; Muguruma, H.; Lee, K.-H.; Karube, I. *Biosens. Bioelectron.* **2004**, *19*, 1667-1672.
- (37) Choi, H.-G.; Boccazzi, P.; Sinskey, A. J.; Laibinis, P. E.; Jensen, K. F. *Polym. Prepr. (Am. Chem. Soc., Div. Polym. Chem.)* **2004**, *45*, 106-107.
- (38) Wang, J.; Muck, A., Jr.; Chatrathi, M. P.; Chen, G.; Mittal, N.; Spillman, S. D.; Obeidat, S. *Lab Chip* **2005**, *5*, 226-230.
- (39) Qu, H.; Wang, H.; Huang, Y.; Zhong, W.; Lu, H.; Kong, J.; Yang, P.; Liu, B. *Anal. Chem.* **2004**, *76*, 6426-6433.
- (40) Henry, A. C.; McCarley, R. L. *J. Phys. Chem. B* **2001**, *105*, 8755-8761.
- (41) Rohr, T.; Ogletree, D. F.; Svec, F.; Frechét, J. M. J. *Adv. Funct. Mater.* **2003**, *13*, 264-270.
- (42) Hozumi, A.; Masuda, T.; Hayashi, K.; Sugimura, H.; Takai, O.; Kameyama, T. *Langmuir* **2002**, *18*, 9022-9027.
- (43) Zhang, J.-Y.; Esrom, H.; Kogelschatz, U.; Emig, G. *J. Adhes. Sci. Technol.* **1994**, *8*, 1179-1210.
- (44) Deleted in proof.
- (45) Liu, J.; Pan, T.; Woolley, A. T.; Lee, M. L. *Anal. Chem.* **2004**, *76*, 6948-6955.
- (46) McCarley, R. L.; Vaidya, B.; Wei, S.; Smith, A. F.; Patel, A. B.; Feng, J.; Murphy, M. C.; Soper, S. A. *J. Am. Chem. Soc.* **2005**, *127*, 842-843.
- (47) Ford, S. M.; Davies, J.; Kar, B.; Qi, S. D.; McWhorter, S.; Soper, S. A. *J. Biomech. Eng.* **1999**, *121*, 13-21.
- (48) Peanasky, J. S.; McCarley, R. L. *Langmuir* **1998**, *14*, 113-123.
- (49) Wang, Y.; Vaidya, B.; Farquar, H. D.; Stryjewski, W.; Hammer, R. P.; McCarley, R. L.; Soper, S. A.; Cheng, Y.-W.; Barany, F. *Anal. Chem.* **2003**, *75*, 1130-1140.
- (50) Huang, X.; Gordon, M. J.; Zare, R. N. *Anal. Chem.* **1988**, *60*, 1837-1838.
- (51) Batich, C. D.; Wendt, R. C. *ACS Symp. Ser.* **1981**, *162*, 221-235.
- (52) Beamson, G.; Briggs, D. *High-Resolution XPS of Organic Polymers: the Scienta ESCA300 Database*; John Wiley & Sons: New York, 1992.
- (53) Johnson, T. J.; Waddell, E. A.; Kramer, G. W.; Locascio, L. E. *Appl. Surf. Sci.* **2001**, *181*, 149-159.
- (54) Suh, K. Y.; Langer, R.; Lahann, J. *Adv. Mater.* **2004**, *16*, 1401-1405.
- (55) Srinivasan, R.; Lazare, S. *Polymer* **1985**, *26*, 1297-1300.
- (56) Ulman, A. *An Introduction to Ultrathin Organic Films: From Langmuir-Blodgett to Self-Assembly*; Academic Press: San Diego, CA, 1991.
- (57) Tseng, A. A.; Chen, K.; Chen, C. D.; Ma, K. J. *IEEE Trans. Electron. Packag.* **2003**, *26*, 141-149.
- (58) Lee, W.; Jin, M.-K.; Yoo, W.-C.; Lee, J.-K. *Langmuir* **2004**, *20*, 7665-7669.
- (59) Fairbank, R. W. P.; Wirth, M. J. *J. Chromatogr. A* **1999**, *830*, 285-291.
- (60) Galloway, M.; Stryjewski, W.; Henry, A.; Ford, S. M.; Llopis, S.; McCarley, R. L.; Soper, S. A. *Anal. Chem.* **2002**, *74*, 2407-2415.
- (61) Rabek, J. F. *Photodegradation of Polymers*; Springer: New York, 1996.
- (62) Lippert, T.; Dickinson, J. T. *Chem. Rev.* **2003**, *103*, 453-485.